PAPER Nr.: 73

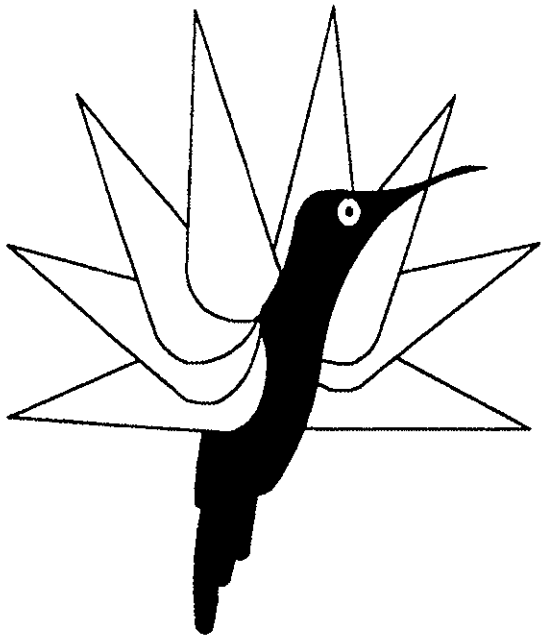

ANALYTICAL AND EXPERIMENTAL INVESTIGATION OF THE EFFECT OF MAST-BENDING COUPLING ON PYLON STABILITY

BY

MITHAT YUCE
JING G. YEN

BELL HELICOPTER TEXTRON, INC.
FORT WORTH, TEXAS, USA

TWENTIETH EUROPEAN ROTORCRAFT FORUM
OCTOBER 4 - 7, 1994 AMSTERDAM

ANALYTICAL AND EXPERIMENTAL INVESTIGATION OF THE EFFECT OF MAST BENDING COUPLING ON PYLON STABILITY

Mithat Yuce
Jing G. Yen
Bell Helicopter Textron, Inc.
Fort Worth, TX U.S.A.

Abstract

The effect of mast-bending coupling on pylon stability of helicopters with a soft-inplane, multibladed rotor is investigated. Mast-bending coupling refers to the mechanism whereby bending of the mast due to hub moments and hub shears produces blade cyclic feathering. The effect of the cyclic feathering on pylon stability depends on pylon frequency, mast flexibility, and geometry of the pitch-link. This paper provides the definition and methods of calculating and measuring mast-bending coupling. The effect of the coupling on pylon stability is demonstrated using analytical and experimental data. Analytical investigations are conducted using Bell Helicopter COPTER and DNAW02 analyses. The experimental data are obtained from flight test of a four-bladed soft-inplane hingeless rotor and from the wind tunnel test of a 1/6-Froude-scale four-bladed soft-inplane bearingless rotor. Results indicate that mast-bending coupling has significant effect on pylon stability. A leading-edge pitch-link is stabilizing while a trailing-edge pitch-link is destabilizing. The destabilizing effect is manifested by the mast flexibility. Studies also show that the effect of mast-bending coupling on ground resonance is insignificant. Furthermore, the effect of mast-bending coupling on pylon stability is not equivalent to a virtual δ_3.

Notation

A_1	Lateral blade cyclic feathering, + right (deg)
B_1	Longitudinal blade cyclic feathering, + forward (deg)
d	Pitch horn moment arm, + for leading edge (in)
K	Coefficient, relates hub translation to hub rotation (in/rad)
r_f	Effective flapping hinge offset without mast flexibility (in)
r_p	Top of the pitch-link radial position (in)
$\Delta\theta$	Incremental blade pitch, + up (rad)
$\Delta\theta_m$	Incremental hub longitudinal rotation, + aft (rad)
$\Delta\theta_0$	Incremental blade pitch due to mast bending at $\psi = 0$ deg (rad)
$\Delta\theta_{90}$	Incremental blade pitch due to mast bending at $\psi = 90$ deg (rad)
$\Delta\phi_m$	Incremental hub lateral rotation, + left (rad)
θ_i	Longitudinal hub rotation in i^{th} fixed system mode
ϕ_i	Lateral hub rotation in i^{th} fixed system mode
δ_i	Participation factor of i^{th} fixed system mode
δ_m	Hub longitudinal translation + aft (in)
δ_3	Pitch flap coupling ,without mast flexibility effect (deg)
ψ	Blade azimuth, zero when the blade is over the tail boom (deg)
γ_0, γ_{90}	Inclination of pitch-link to the control plane (deg) (see Fig 5)

Introduction

The effect of pylon/swashplate couplings on pylon stability has been well understood (Refs. 1 and 2). Depending on the phasing of the swashplate coupling (i.e., the swashplate leads or lags the pylon motion), the rotor aerodynamic damping tends to stabilize the pylon motion when the swashplate leads and to destabilize the pylon motion when the swashplate lags. If the swashplate follows the pylon, it is called "mast stabilized"; if the swashplate remains in space when the pylon rocks, it is called "space stabilized." Hence, an over-mast-stabilized pylon control coupling is stabilizing and a space-stabilized or over-space-stabilized swashplate coupling is destabilizing. Since an over-mast-stabilized coupling is not desirable for good handling qualities, a swashplate coupling between the mast-stabilized and the space-stabilized conditions is usually selected for actual pylon designs.

Mast-bending coupling refers to the mechanism whereby bending of the mast due to hub moments and hub shears produces blade cyclic feathering. With given hub loads, the magnitude and phase of the blade feathering depend

on the flexibility of the mast and on pitch-link geometry. The significance of mast-bending coupling on rotor stability was first discovered on the YAH-64. During the early development of the YAH-64 Apache helicopter, an advancing whirl mode instability was predicted and encountered on the whirl tower test (Ref. 3). This instability was a direct result of the coupling between the rotor blade cyclic feathering and bending of a relatively soft mast. An examination of the YAH-64 whirl instability using a simplified linear analysis was recently performed by Kunz (Ref. 4). Another recent paper by Loewy and Zotto (Ref. 5) included blade feathering/mast-bending coupling in an investigation of ground and air resonance. All these studies (Refs. 1 through 5), however, did not address the effect of mast-bending coupling on pylon stability.

The significance of mast-bending coupling on the pylon stability of helicopters was first recognized at Bell during developmental flight testing of Bell Model 400. The Model 400 was a four-bladed hingeless soft-inplane rotor. The aircraft was tested at both leading-edge and trailing-edge pitch-horn positions. Flight test data clearly demonstrated a weak pylon stability when the aircraft was tested at the trailing-edge position. Acceptable pylon stability margin was achieved when the pylon frequency was raised. Wind tunnel testing of a 1/6-Froude-scale model of a four-bladed, soft-inplane bearingless rotor was conducted (Ref. 6). Pylon stabilities were investigated by testing four pitch-horn/pitch-link locations: inboard and outboard trailing-edge positions and inboard and outboard leading-edge positions. A positive trend of pylon damping was measured when the pitch-link location was moved from the trailing edge to the leading edge. Correlation of the model data using a comprehensive analysis methodology is briefly discussed in Ref. 7. Through the flight testing of the Model 400 helicopter and the wind tunnel testing of the 1/6-Froude-scale model, the single design parameter that significantly affects the pylon damping was identified to be the sign of mast-bending coupling.

This paper provides a definition of mast-bending coupling, methods of measuring and calculating the coupling terms, and a document of pylon stability correlation using flight test and wind tunnel data. The effect of mast-bending coupling on ground resonance is discussed. This paper represents, to the authors' best knowledge, the first attempt at providing a comprehensive documentation of the effect of mast-bending coupling on pylon stability.

1. Background

The Bell Model 400 was an experimental light twin helicopter with a four-bladed soft-inplane hingeless main rotor. An isometric view of the helicopter is shown in Fig. 1. The aircraft was extensively flight tested between 1984 and 1985. During this period, a weak pylon stability margin in hover was encountered when the aircraft was tested at a trailing-edge pitch-horn configuration. Acceptable pylon stability margin was achieved when the pylon frequency was raised and the pitch-horn was moved from the trailing edge to the leading edge. Relevant dynamic components of the aircraft are briefly described in the following paragraphs.

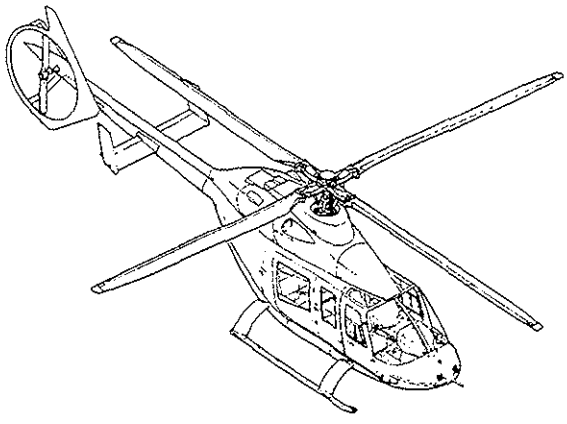

4G970
Fig. 1. Isometric view of Bell Model 400.

The helicopter had all-composite main rotor blades. The primary parameters of the blades are listed in Table 1. The main rotor hub consisted of a composite yoke, an elastomeric lead-lag damper, and feathering bearings. The blades were attached to the yoke via a grip assembly (Fig. 2). Provisions were made for the pitch-horns to be attached at the leading or trailing edge of the blade. In addition, the radial location of the pitch-link attachment point to the pitch-horn was adjustable. Seven different pitch-link attachment points could be used for leading- or trailing-edge configurations. In Fig. 3, variable pitch-link attachment points are shown schematically.

In Fig. 4, the pylon support system of the helicopter is shown. The transmission is mounted on two side beams via four elastomeric soft mounts, with the side beams rigidly attached to the roof. The bottom of the transmission case is

Table 1. Model 400 main rotor blade parameters

Parameter	Units	Value
Main rotor radius	ft	18.5
Thrust-weighted blade chord	ft	0.8858
Rotor speed	rpm	383
Rotor weight	lb/blade	97.292
First moment of inertia	slug-ft/blade	17.865
Second moment of inertia	slug-ft^2/blade	205.192
Effective flapping hinge offset*	ft	0.75
Effective lag hinge offset	ft	1.583
Lock number	–	6.093

*Calculated without mast flexibility.

also attached to the roof through two fore-and-aft elastomeric springs. The mast is hollow,

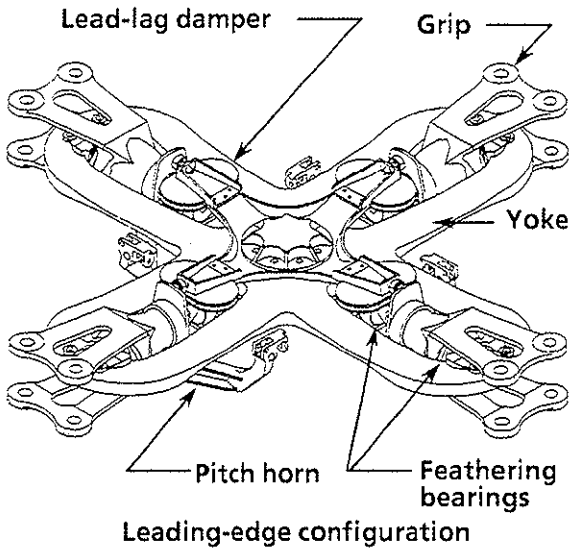

4G971

Fig. 2. Model 400 hub assembly.

rotating, and soft in bending (approximately 23,356 in-lb/deg).

Three prototypes of the Model 400 (Ship 1, Ship 2, and Ship 3) were flown during the developmental flight testing. The experimental data

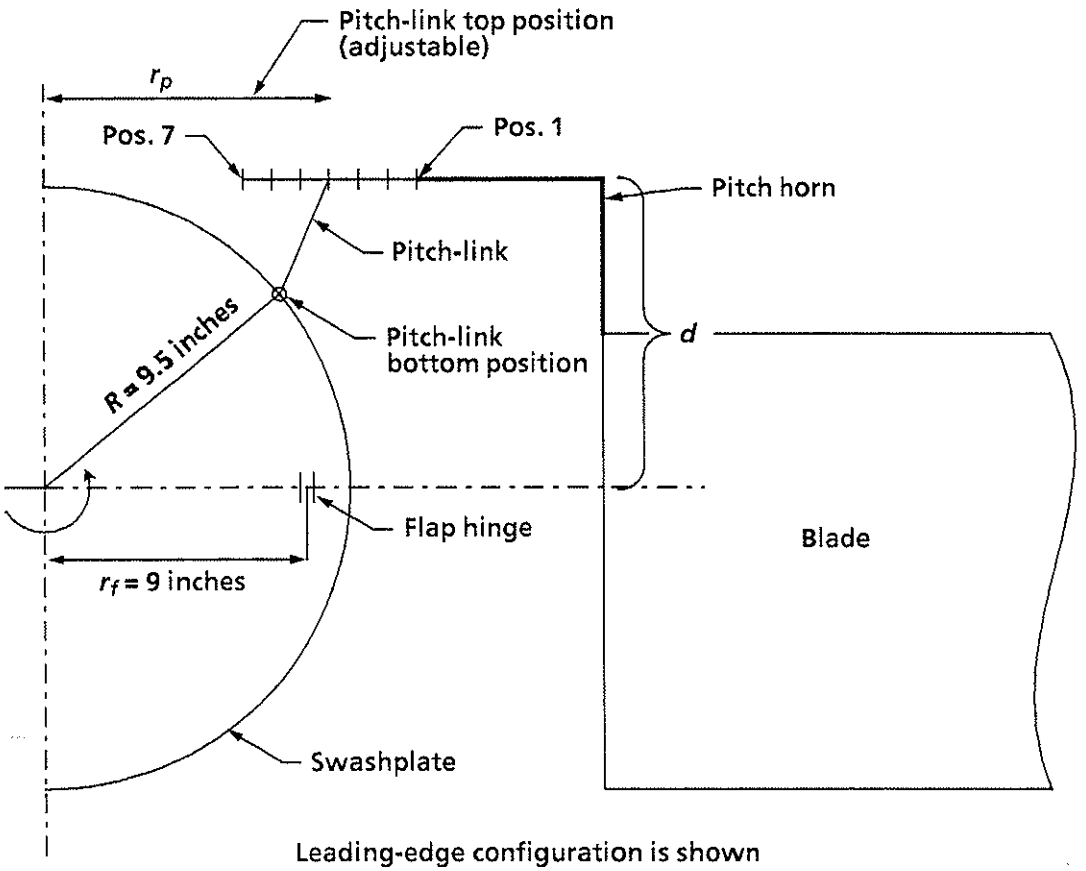

4G973

Fig. 3. Schematic illustration of the Model 400 adjustable pitch-horn.

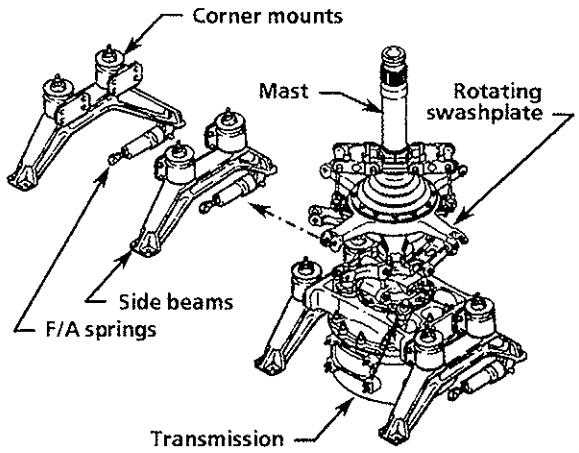

4G972
Fig. 4. Model 400 pylon support and rotating control system.

presented in this paper is from all three of these prototype helicopters. The important hardware variation between these prototypes, from the pylon stability point of view, was the spring rates of the elastomeric pylon corner mounts and the lead-lag dampers, which are defined in Table 2. Table 2 also shows the pylon and the lead-lag mode frequencies for each prototype helicopter.

2. Definition of the Mast Bending Coupling

The blade cyclic feathering due to the mast bending can be represented as follows:

$$\Delta\theta = -\Delta\theta_m\left(\frac{\partial A_1}{\partial\theta_m}\cos\psi+\frac{\partial B_1}{\partial\theta_m}\sin\psi\right) -\Delta\phi_m\left(\frac{\partial A_1}{\partial\phi_m}\cos\psi+\frac{\partial B_1}{\partial\phi_m}\sin\psi\right) \quad (1)$$

where $\Delta\theta$ is the blade pitch variation around the azimuth due to $\Delta\theta_m$ and $\Delta\phi_m$, longitudinal and lateral mast bending with respect to the control plane, and A_1, B_1 are the lateral and longitudinal cyclic control inputs. The partial derivative coefficients in Equation (1) are the mast-bending coupling terms which describe the magnitude of cyclic feathering due to a unit rotation at the top of the mast in the lateral and longitudinal directions. The magnitude and sign of these coupling terms depend on the geometry of the rotating control system, as explained below.

In Fig. 5a, a rotor blade with a trailing-edge pitch-horn configuration is shown at $\psi=0$ deg. It is assumed that top of the mast is tilted aft by $\Delta\theta_m$ radians and translated by δ_n inches due to the hub loads. Assuming small deflections, the blade feathering due to the mast deflection is approximated as

$$\Delta\theta_0 = \frac{r_p}{d}\Delta\theta_m - \frac{\delta_m}{d\tan\gamma_0} \quad \text{or}$$
$$\Delta\theta_0 = \left(\frac{r_p}{d}-\frac{K}{d\tan\gamma_0}\right)\Delta\theta_m \quad (2)$$

and, therefore,

$$\frac{\partial A_1}{\partial\theta_m} = -\left(\frac{r_p}{d}-\frac{K}{d\tan\gamma_0}\right) \quad (3)$$

where r_p and d are the radial location and the moment arm of the pitch horn, respectively, as shown in Fig. 5a. The sign of d is positive for the leading-edge pitch horn. The angle γ_0 is the inclination angle of the pitch-link to the control plane, as shown in the figure, where K is a coefficient that relates the hub translation to the

Table 2. Elastomeric springs and dampers used on Model 400 prototype ships and their effects on the pylon and lead-lag mode frequencies.

		Ship 1	Ship 2	Ship 3
Corner mount spring rate (dynamic)	lb/in	2,600	4,500	4,500
F/A restraint spring rate (dynamic)	lb/in	13,700	13,700	13,700
Pylon roll mode frequency	Hz	4	5.25	5.25
Pylon pitch mode frequency	Hz	4.5	6.2	6.2
Lead-lag damper spring rage (nominal)	lb/in	16,000	22,000	16,000
Lead-lag mode frequency (at 383 rpm)	/rev	0.59	0.63	0.59

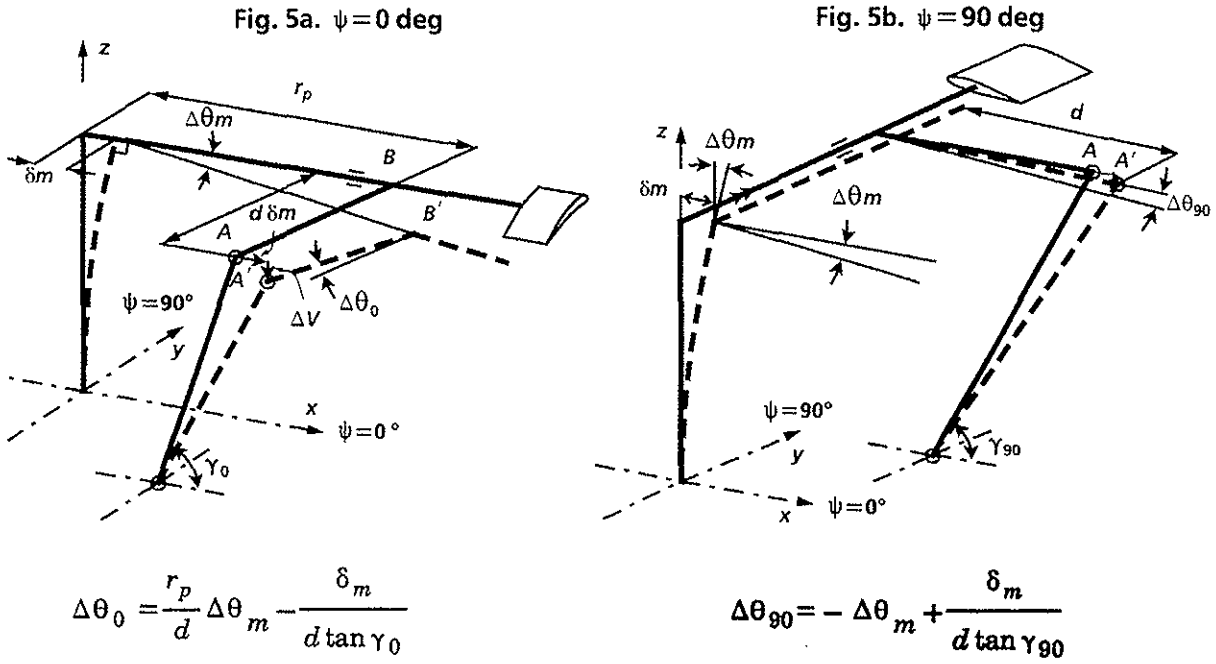

4G969

Fig. 5. Schematic illustration of mast-bending coupling (trailing-edge configuration).

hub rotation. For the Model 400 mast, the value of K was 17.85 in/rad. Note that the sign change between Equations 2 and 3 is due to fact that A_1 is positive when the blade at $\psi=0$ deg pitches down.

Similarly, the blade is shown at $\psi=90$ deg in Fig. 5b. The blade feathering due to the mast deflection is approximated as

$$\Delta\theta_{90} = -\Delta\theta_m + \frac{\delta_m}{d\tan\gamma_{90}} \quad \text{or}$$

$$\Delta\theta_{90} = -\left(1 - \frac{K}{d\tan\gamma_{90}}\right)\Delta\theta_m \tag{4}$$

and, therefore,

$$\frac{\partial B_1}{\partial\theta_m} = \left(1 - \frac{K}{d\tan\gamma_{90}}\right) \tag{5}$$

where γ_{90} is the pitch-link inclination angle to the control plane, as shown in Fig. 5b.

Because of the symmetry of the mast, the blade pitch due to the mast lateral deflection may be approximated as

$$\frac{\partial A_1}{\partial\phi_m} = \frac{\partial B_1}{\partial\theta_m} = \left(1 + \frac{K}{d\tan\gamma_0}\right) \tag{6}$$

and

$$\frac{\partial B_1}{\partial\phi_m} = -\frac{\partial A_1}{\partial\theta_m} = \left(\frac{r_p}{d} - \frac{K}{d\tan\gamma_{90}}\right) \tag{7}$$

It should be noted that for pitch-links perpendicular to the control plane, the second terms in the parentheses are eliminated. Thus the equations are further simplified. The above formulations represent only a first-order approximation of mast-bending coupling terms, which was exclusively used in this paper and was found adequate to explain the pylon stability characteristics.

Mast-bending coupling terms can also be experimentally determined by a static hub pull test. A representative static inplane force is applied to the hub while the helicopter is secured on the ground. The resultant slope at the top of the mast is measured relative to the swashplate; then the pitch angle of the reference blade is measured around the azimuth. With the knowledge of the reference

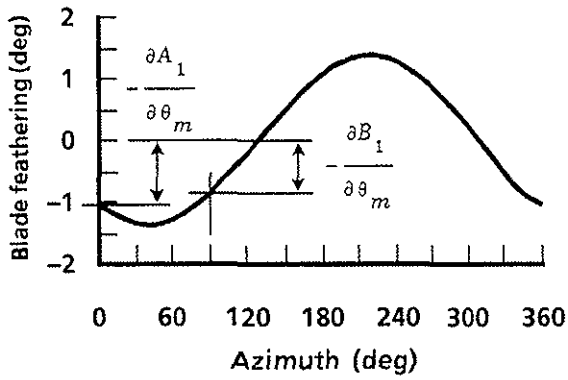

4H584

Fig. 6. Blade feathering around the azimuth for 1-deg mast tilted aft: trailing-edge pitch-horn is shown.

blade-pitch-angle variation with azimuth and the total deflection of the mast, the mast-bending coupling terms can easily be inferred. In Fig. 6 is shown a typical blade feathering due to mast tilting of 1 deg aft versus azimuth for a trailing-edge pitch-horn configuration. The $\partial A_1/\partial\theta_m$ and $\partial B_1/\partial\theta_m$ coupling terms will be equal to the negative values of the blade feathering at $\psi=0$ deg and $\psi=90$ deg, respectively, as shown in the figure.

3. Variation of Mast Bending Coupling and δ_3 with Pitch-Horn Locations

As discussed earlier, the Model 400 was equipped with an adjustable pitch-horn which had seven adjustment points for the radial distance of pitch-link attachment point r_p (see Fig. 3). The No. 7 adjustment point was the most inboard and the No. 1 point was the most outboard location. Using the previously discussed formulation (Eqs. 6 and 7), the mast-bending coupling terms for each of the adjustment points for the leading-edge and trailing-edge pitch-horn configurations are calculated and listed in Table 3, together with the

Table 3. Variation of mast-bending coupling and δ_3 with pitch-link attachment points.

Pitch-link attachment point	r_p (in)	d (in)	γ_0 (deg)	γ_{90} (deg)	$\frac{\partial A_1}{\partial \theta_m}$ (deg/deg)	$\frac{\partial B_1}{\partial \theta_m}$ (deg/deg)	$\delta_3 = -\tan^{-1}\frac{\Delta\theta}{\Delta\beta}$ (deg)
LEADING-EDGE PITCH-HORN CONFIGURATION							
1	10.65	7	80.10	87.44	−1.07	0.89	13.28
2	10.01	7	81.92	87.44	−1.06	0.89	8.19
3	9.38	7	83.74	87.44	−1.05	0.89	3.09
4	8.74	7	85.58	87.44	−1.05	0.89	−2.12
5	8.10	7	87.42	87.44	−1.04	0.89	−7.35
6	7.46	7	89.25	87.44	−1.03	0.89	−12.41
7	6.82	7	91.10	87.44	−1.02	0.89	−17.27
TRAILING-EDGE PITCH-HORN CONFIGURATION							
1	10.65	−7	80.10	92.55	1.07	0.89	−13.28
2	10.01	−7	81.92	92.55	1.06	0.89	−8.19
3	9.38	−7	83.74	92.55	1.05	0.89	−3.09
4	8.74	−7	85.58	92.55	1.05	0.89	2.12
5	8.10	−7	87.42	92.55	1.04	0.89	7.35
6	7.46	−7	89.25	92.55	1.03	0.89	12.41
7	6.82	−7	91.10	92.55	1.02	0.89	17.27

Note that $\frac{\partial B_1}{\partial \phi_m} = -\frac{\partial A_1}{\partial \theta_m}$ and $\frac{\partial A_1}{\partial \phi_m} = \frac{\partial B_1}{\partial \theta_m}$ due to mast symmetry.

corresponding values of r_p, γ_0, γ_{90}. It can be seen that the magnitude and sign of the $\partial B_1/\partial\theta_m$ coupling term do not change with the pitch-horn adjustment points or with the pitch-horn configuration as the leading edge or trailing edge. This is because the $\partial B_1/\partial\theta_m$ term is a function of d and $\tan\gamma_{90}$, which do not change with the pitch-link spanwise location (see Equation 6). On the other hand, the signs of both d and $\tan\gamma_{90}$ change when the pitch horn is moved from the leading edge to the trailing edge. Since $\partial B_1/\partial\theta_m$ is a function of the product of d and $\tan\gamma_{90}$, changing sign for d and $\tan\gamma_{90}$ simultaneously does not change the sign for $\partial B_1/\partial\theta_m$. The same argument is valid for the $\partial A_1/\partial\phi_m$ term, since $\partial A_1/\partial\Phi_m = \partial B_1/\partial\theta_m$, due to the symmetry of the mast.

On the other hand, the magnitude of the $\partial A_1/\partial\theta_m$ term varies very slightly with the pitch-link spanwise location. This insensitivity of the coupling term to the adjustment points is due to the fact that $\partial A_1/\partial\theta_m$ is a function of r_p and $\tan\gamma_0$, which affect the coupling term in an opposite direction as the pitch-link attachment point changes (see Equation 7). The effect of the pitch-horn configuration on this coupling term is a sign change, positive for the trailing edge, due to the sign of the pitch-horn moment arm d. It can also be noted that $\partial B_1/\partial\Phi_m = -\partial A_1/\partial\theta_m$, due to the symmetry of the mast.

Another coupling term that is affected by the pitch-link attachment point is the blade pitch-flap coupling, δ_3, which is defined as

$$\delta_3 = -\tan^{-1}\left(\frac{\Delta\theta}{\Delta\beta}\right) \qquad (8)$$

where β is the blade flapping with respect to the mast (the mast is assumed to be infinitely rigid) (positive up), and θ is the blade pitch (positive up).

It can be shown that δ_3 may be approximated by

$$\delta_3 = -\tan^{-1}\left(\frac{r_f - r_p}{d}\right) \qquad (8a)$$

where r_f is the equivalent flapping hinge offset of the blade, as shown in Fig. 3. Using the above formula, the values of δ_3 for each pitch-link location are also listed in Table 3. It can be seen that, using the full range of the adjustable pitch-horn, the value of δ_3 can be varied from -13.28 deg to 17.27 deg for both leading- and trailing-edge configurations.

4. Mast Bending Coupling and δ_3 Effect on Pylon Stability

During the developmental flight testing of the Model 400, the aircraft was tested at different pitch-link configurations; thus, the magnitude and sign of δ_3 and the sign of mast-bending coupling were changed. Although the initial intention for this exercise was to improve the handling qualities of the aircraft, the emphasis was shifted, to a study of the effects of mast-bending coupling and δ_3 on pylon stability, after encountering weak stability margins, as explained in the following.

The problem was first noticed during pylon stability testing on Ship 1 when the pitch-horn configuration was changed from leading-edge position No. 4 to trailing-edge position No. 7 (Fig. 3). When a longitudinal cyclic control pulse was used to excite the pylon pitch mode in hover at 100% rotor speed (383 rpm), the pylon responded both in pitch and roll direction with relatively large amplitude. The amplitude of pylon oscillation was higher in the roll direction, and oscillated in a limit cycle fashion until the pilot set the aircraft down. A significantly large blade lead-lag motion was also observed in this event. The frequency of the lead-lag motion was 2.5 Hz in the rotating system. This corresponds to 1/rev minus the pylon frequency, as can be seen from the yoke chord-bending moment time history in Fig. 7. Note that the lead-lag mode natural frequency was 0.59/rev (3.77 Hz in the rotating system). See Table 2. The response of the pylon resembled that of a dynamic system with zero damping, as can be seen from the time history shown in Fig. 7. After that the test was repeated for trailing-edge pitch-horn locations No. 5 and No. 4 (moving outboard). In Fig. 8, the measured pylon roll mode damping is plotted at each pitch-link location against corresponding δ_3 values. Also shown are the pitch-link location numbers. Since mast-bending coupling is not sensitive to pitch-link location, as shown in Table 3, Fig. 8 indicates that increasing value of δ_3, in the positive direction, has a strong destabilizing effect on pylon mode damping. Note that in this paper, δ_3 is positive for flap-up, pitch-down with no mast-bending flexibility.

Initially such a destabilizing effect of δ_3 could not be predicted analytically. The problem was incorrect modeling of mast-bending coupling,

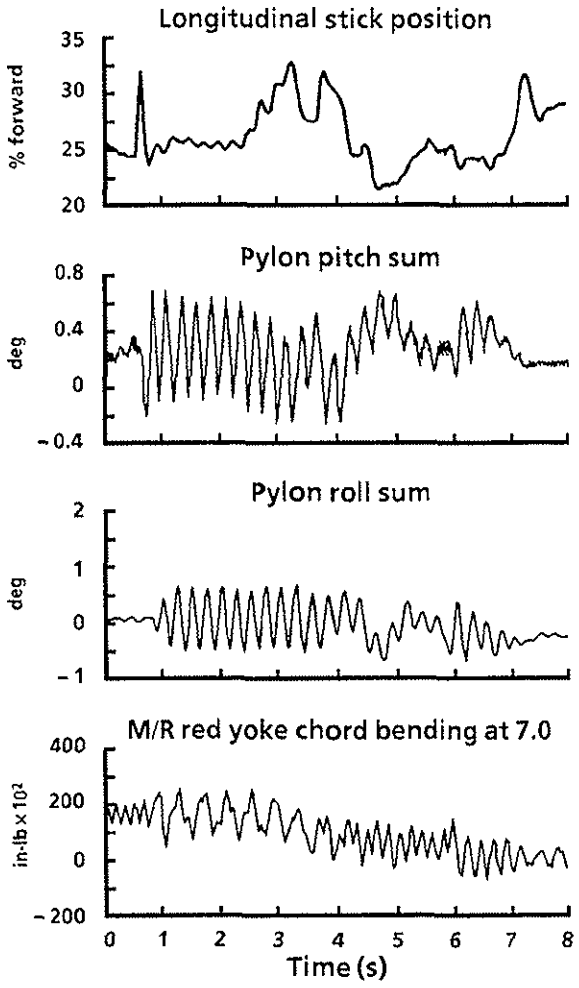

4G968

Fig. 7. Model 400 Ship 1 pylon response to a longitudinal cyclic pulse excitation in hover: Trailing-edge pitch-horn position No. 7; rotor speed = 383 rpm; pylon roll mode frequency = 4.0 Hz;16,000 lb/in lead-lag dampers; gross weight = 5,000 lb.

which was corrected later. With this correction, DNAW02, which is one of Bell's ground and air resonance analysis tools, could capture the measured damping trend (as shown in Fig. 8). A brief description of DNAW02 and modeling of the coupling terms will be given in the later paragraphs.

In Fig. 9, DNAW02-predicted frequencies and damping of the various modes of the Ship 1 in hover are plotted against rotor speed. Data in the figure represent trailing-edge pitch-link location No. 4. Measured data are also shown. It can be seen that calculated and measured pylon roll mode damping sharply reduces with rotor speed. The correlation is not excellent; however, the theory predicted the trend and the instability closely. The analysis indicated that the reason for the sharp damping reduction was

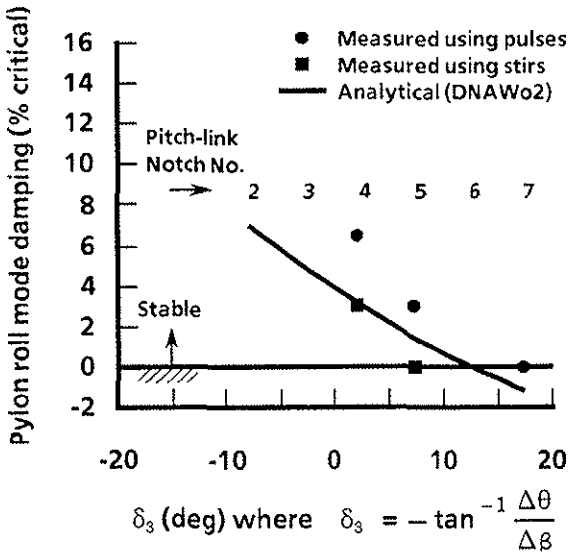

4G977

Fig. 8. Model 400 Ship 1 pylon mode damping variation with δ_3 in hover: Trailing-edge pitch-horn configurations; rotor speed = 383 rpm, pylon roll mode frequency = 4.0 Hz, 16,000 lb/in lead-lag dampers; gross weight = 5,000 lb

the strong coupling between pylon roll and the regressing inplane mode. This reduction was aggravated by the unfavorable sign of mast-bending coupling, even though resonance frequencies of these modes were still well separated at around 410 rpm, where the neutral stability was measured or predicted (as shown in Fig. 9).

In an attempt to increase the stability margin of the helicopter in hover, Ship 2 was modified. The modification included increasing the spring rate of the elastomeric pylon corner mounts from 2600 lb/in to 4500 lb/in and increasing the spring rate of the lead-lag dampers from 16,000 lb/in to 22,000. lb/in. With these changes, pylon roll mode frequency was increased to 5.25 Hz from 4 Hz and the regressing inplane mode frequency was reduced to 2.36 Hz from 2.6 Hz at 383 rpm. Thus, greater frequency separation between these two modes was provided (see also Table 2). The aircraft was tested for hover stability with different trailing-edge pitch-link locations. The results are summarized in Fig. 10 for 106% overspeed or 405 rpm, showing pylon roll mode damping versus δ_3 and the corresponding pitch-link locations. DNAW02 results are also shown in the figure. Both test and the analytical results indicated a significant improvement in pylon damping compared to that of the Ship 1 configuration. However the destabilizing effect of

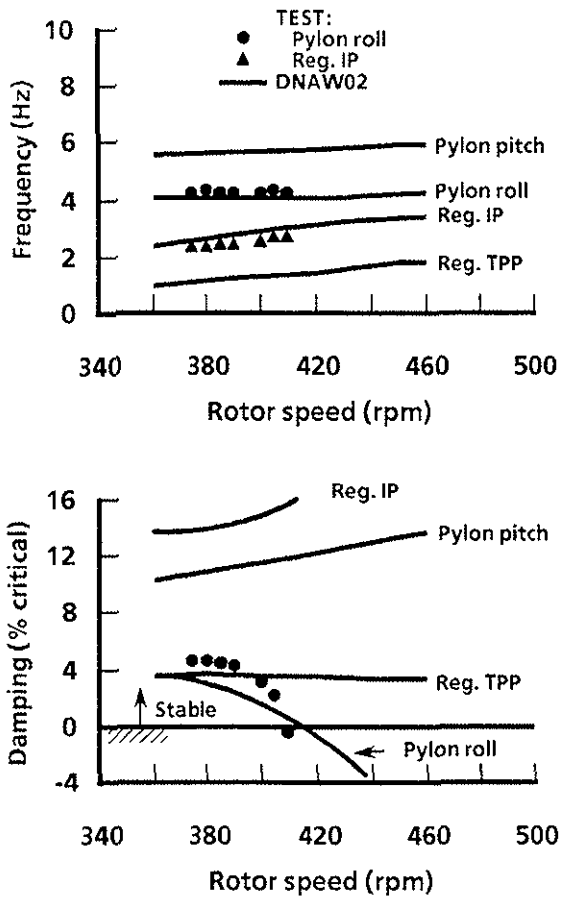

4G981

Fig. 9. Effect of rotor speed on the hover stability characteristics of Model 400 Ship 1: Trailing-edge pitch-horn position No. 4; 16,000 lb/in lead-lag dampers; gross weight = 4,500 lb.

δ_3 on the pylon mode had the same characteristic as that in Ship 1. Pylon roll mode damping was still decreasing while δ_3 was increasing. The slope of this decrease, however, was much shallower than that with the original softer pylon mount and softer lead-lag damper spring rates. In Fig. 11, the measured and predicted effect of the main rotor speed on the stability characteristic of the aircraft in hover is shown for trailing-edge pitch-link position No. 4. By comparing Fig. 11 and Fig. 9, a significant increase in pylon roll mode damping can be observed primarily due to increases in the frequencies of the pylon and the lead lag modes. It can also be seen that DNAW02 predicts the effect of the modification reasonably well.

Parallel to Ship 2, Ship 3 was flight tested with leading-edge pitch-horn configuration. Dynamic components of both aircraft were identical except for lead-lag dampers. Ship 3 was installed with softer damper spring rates of 16,000 lb/in compared to 22,000 lb/in for Ship 2

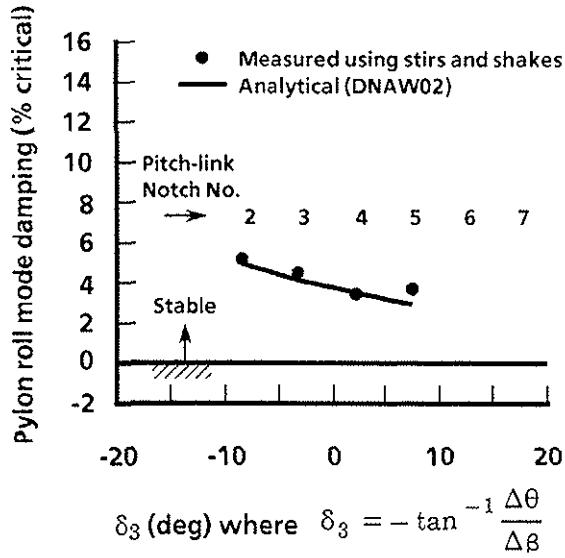

4G976

Fig. 10. Model 400 Ship 2 pylon mode damping variation with δ_3 in hover: Trailing-edge pitch-horn configurations; rotor speed = 405 rpm; pylon roll mode frequency = 5.25 Hz; 22,000 lb/in lead-lag dampers; gross weight = 4,500 lb.

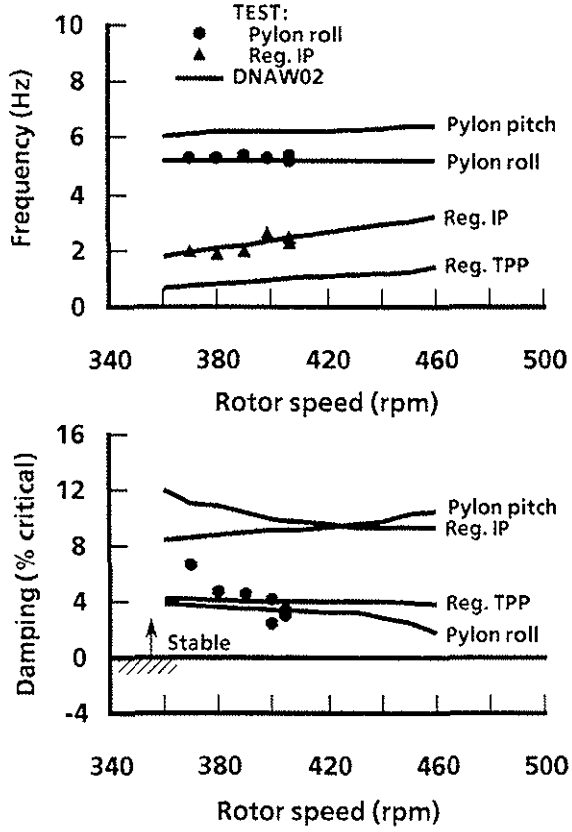

4G979

Fig. 11. Effect of rotor speed on the hover stability of Model 400 Ship 2: Trailing-edge pitch-horn position No. 4; 22,000 lb/in lead-lag dampers; grossweight = 4,500 lb.

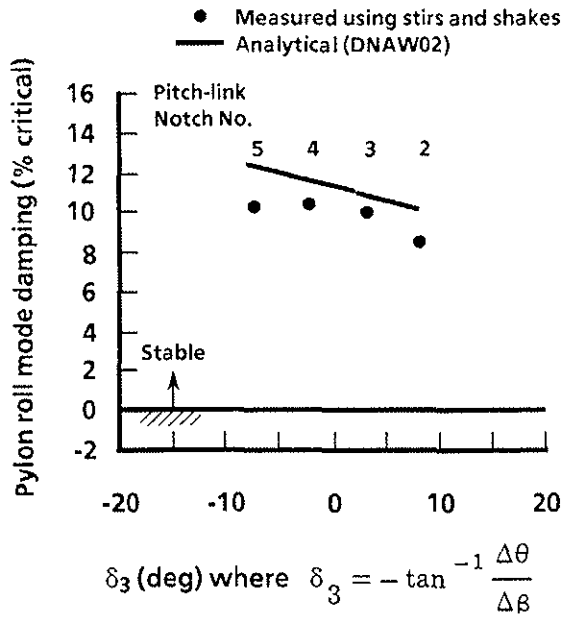

4G978

Fig. 12. Model 400 Ship 3 pylon roll mode damping variation with δ_3 in hover: Leading-edge pitch-horn configurations; rotor speed = 405 rpm; pylon roll mode frequency = 5.25 Hz; 16,000 lb/in lead-lag dampers; gross weight = 5,500 lb.

(see Table 2). Ship 3 had also adjustable pitch-link radial location.

In Fig. 12, the measured and predicted pylon roll mode damping of Ship 3 is plotted versus δ_3 for the pitch-link locations tested. Comparison of Fig. 12 and Fig. 10 shows a substantial increase in pylon damping (nearly doubled) when the pitch-link was moved from the trailing edge to the leading edge. Although lead-lag dampers were not identical between these two aircraft, the increase in pylon damping is mostly due to the change in sign for two mast-bending coupling terms, $\partial B_1/\partial\phi_m$ and $\partial A_1/\partial\theta_m$. The data in these figures also indicated that the DNAW02 analysis results correlate well with the test data.

Effect of the main rotor speed on hover stability of Ship 3 is shown in Fig. 13 for leading-edge pitch-horn position No. 3. Again, comparison of Fig. 13 and Fig. 11 indicates a marked increase in pylon roll mode damping, primarily due to the change in pitch-horn configuration from trailing edge to leading edge.

In order to show that the increase in damping is mostly due to the mast-bending coupling terms, the DNAW02 analysis was run for the leading-edge and trailing-edge pitch-horn

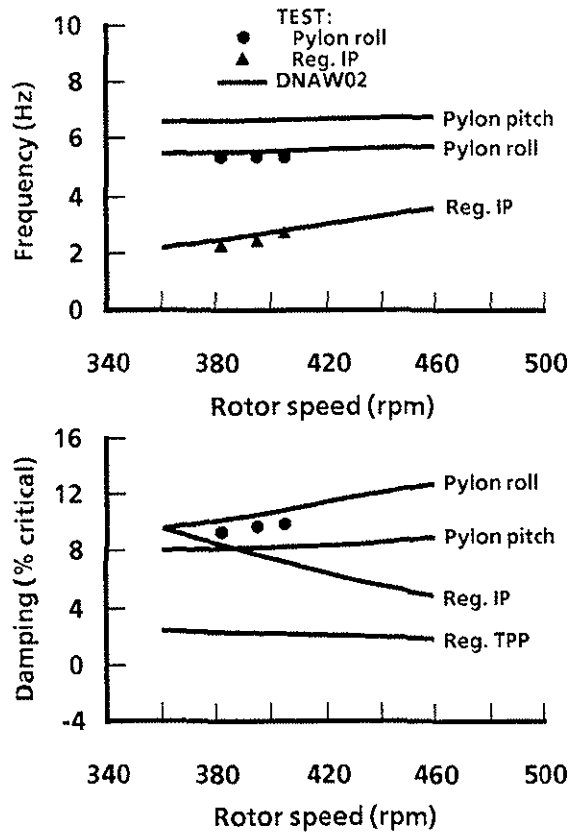

4G980

Fig. 13. Effect of rotor speed on the hover stability characteristics of Model 400 Ship 3: Leading-edge pitch-horn position No. 3; 16,000 lb/in lead-lag dampers; gross weight = 5,500 lb.

configurations by changing only the sign of mast-bending coupling term and keeping all the other input parameters identical. The result of this exercise is plotted in Fig. 14, which clearly shows the strong stabilizing or destabilizing effect of the mast-bending coupling terms.

5. DNAW02 Analysis

DNAW02 is one of Bell's ground and air resonance stability analysis programs that was extensively used in this study. DNAW02 is an eigenvalue analysis. For an isotropic rotor, the analysis utilizes the multiblade coordinate transformation to eliminate the time-varying coefficients. A non-isotropic rotor option is also available, which computes time-dependent eigenvectors. The rotor model consists of three to seven identical, equally spaced, rigid-hinged blades that may have different spring and/or damper values for lead-lag and flapping restraints. The fixed system is represented by modal parameters, up to six modes. Blade aerodynamics are modeled using 2-D quasi-static

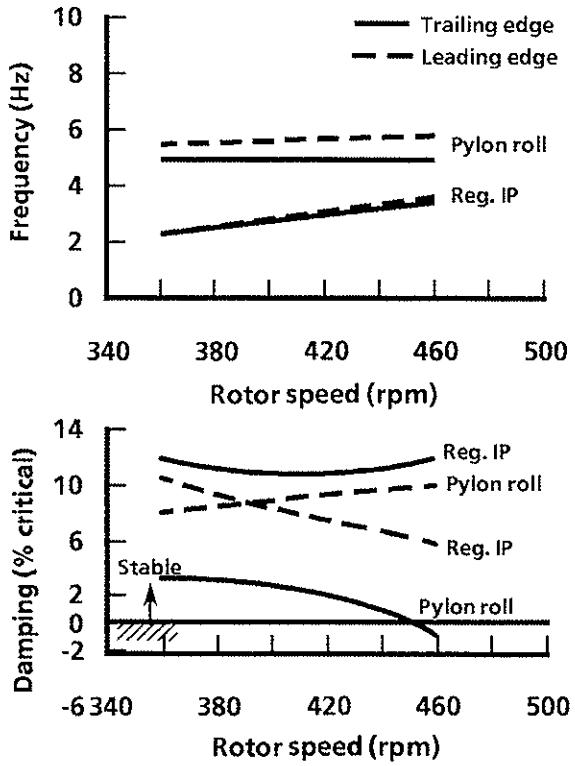

4G983

Fig. 14. Effect of the sign of mast-bending coupling terms on pylon stability in hover.

strip theory and table look-up. The kinematic coupling terms, such as pitch-flap, pitch-lag, pitch-cone, and pylon-swashplate coupling are modeled in blade aerodynamics.

Before the pylon stability problem of the Model 400 was encountered in DNAW02, the mast-bending coupling term was modeled via an equivalent δ_3. This was done by calculating an effective flapping-hinge offset which reflects the hub and mast flexibility. For example, the flapping-hinge offset of Model 400 with and without mast flexibility effects are 5.38 and 9 inches, respectively. Experience with the Model 400 showed the inadequacy of this modeling approach in stability analysis when the destabilizing effect of the trailing-edge pitch-horn configuration could not be predicted. In Fig. 15 the pylon mode damping computed by DNAW02 analysis using the equivalent δ_3 modeling approach is shown for leading-edge and trailing-edge configurations, position No. 4. In this figure, rotor and fixed system parameters reflect the Ship 3 configuration. It can be seen that the damping is increasing with the rotor speed for the both configurations, and the trailing-edge configuration has higher damping. As was discussed earlier, the damping trend shown in Fig. 15 was opposite to that measured in the flight test.

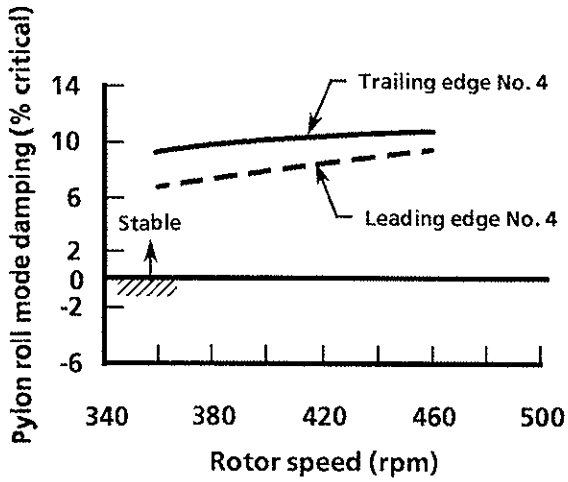

4G982

Fig. 15. Effect of representing mast flexibility via equivalent δ_3 on pylon mode damping prediction in hover.

There was a fundamental problem when the mast flexibility effect was represented by an equivalent δ_3. The following two terms were absent from the mathematical representation: $\partial A_1/\partial \phi_m$ and $\partial B_1/\partial \theta_m$. As a result, the effects of the hub shears and moments were not rigorously represented.

In the present methodology, which correlates well with flight test, mast-bending coupling represents the mast flexibility while the pitch-flap coupling represents the hub flexibility. These two couplings are separately modeled in the DNAW02 analysis. The blade feathering due to mast bending coupling is represented as

$$\Delta\theta = (\sin\psi, \cos\psi)\begin{bmatrix} \frac{\partial B_1}{\partial \theta_m} & \frac{\partial B_1}{\partial \phi_m} \\ \frac{\partial A_1}{\partial \theta_m} & \frac{\partial A_1}{\partial \phi_m} \end{bmatrix} \times \begin{bmatrix} \theta_1 & \theta_2 & \cdots & \theta_n \\ \phi_1 & \phi_2 & \cdots & \phi_n \end{bmatrix} \begin{Bmatrix} \delta_1 \\ \delta_2 \\ \vdots \\ \delta_n \end{Bmatrix} \quad (9)$$

where θ_n and ϕ_n are the mast longitudinal and lateral rotational mode shapes at the hub with respect to the control plane in the n^{th} fixed system mode, and δ_n is the modal participation factor of the n^{th} fixed system mode. The effects of the hub shears and moments are seen on the modal participation factors.

6. Test Correlation: 1/6-Froude-scale Model

Further studies on the effects of trailing- and leading-edge pitch-horn configuration on pylon stability were made on a one-sixth-scale Froude 4-bladed soft inplane bearingless model rotor in a wind tunnel (Ref. 6). The results using data from the wind tunnel model also indicated that leading-edge pitch-horn configuration has a stabilizing effect on pylon mode. It should also be noted that the wind tunnel model employed a stiff mast and stiff pylon mounts. Adequate pylon damping was measured with the trailing-edge pitch-horn. In this work, COPTER, Bell's flight simulation comprehensive program (Ref. 7), was used as the analytical tool. Fig. 16, which was reproduced from Ref. 6, shows effect of pitch-horn location on pylon roll mode damping. In the figure, both analytical and experimental data are presented. It can be seen that the COPTER results correlate well in trend with the measured data. Mast-bending coupling terms in COPTER analysis were also modeled separately from the pitch-flap coupling to achieve this level of correlation.

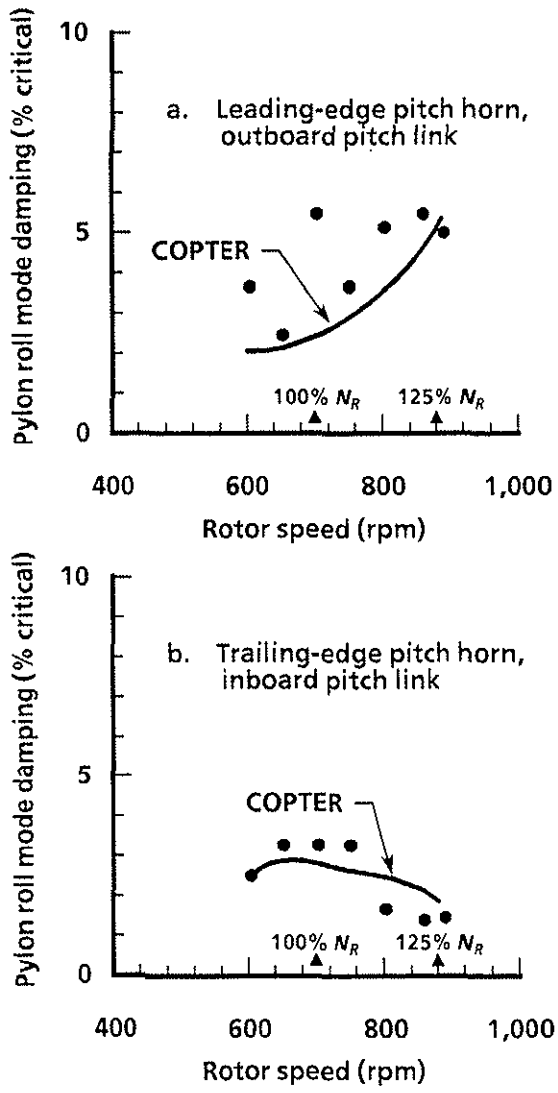

4G975
Fig. 16. Measured and predicted pylon roll mode damping in hover for 1/6-Froude-scale model.

7. Mast-Bending Coupling Effect on Ground Resonance

The Model 400 had an adequate ground resonance stability margin which was not sensitive to the pitch-horn configuration. These results indicate that mast-bending coupling does not have a significant effect on ground resonance stability. DNAW02 analysis results have also confirmed this observation, as shown in Figs. 17 and 18. Figure 17 shows the ground resonance stability characteristics of Ship 3 for trailing-edge pitch-horn configuration No. 4 and with zero thrust. The analytical model included five fixed system modes, three fuselage

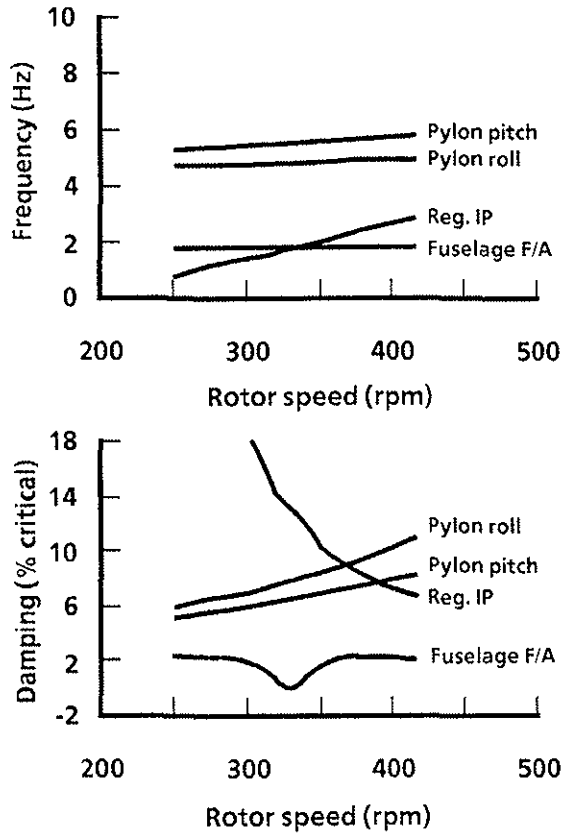

4G986
Fig. 17. Effect of the mast-bending coupling terms on Model 400 Ship 3 ground resonance stability: DNAW02 result for trailing edge pitch-horn position No. 4.

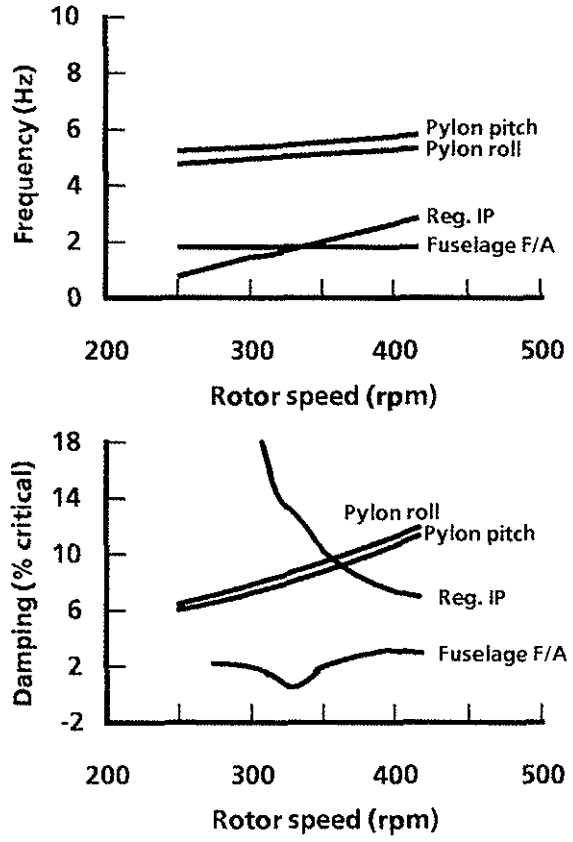

4G987

Fig. 18. Effect of the mast-bending coupling terms on Model 400 Ship 3 ground resonance stability: DNAW02 result for the leading-edge pitch-horn position No. 4.

modes (roll, pitch, and longitudinal shuffle on the landing gear), and two pylon modes (pitch and roll). However, in the figure, only the longitudinal shuffle (least damped), regressing inplane, and the pylon modes are shown for clarity. Similarly, Fig. 18 shows the ground resonance stability characteristics for leading-edge configuration No. 4. Comparison of Fig. 17 and Fig. 18 shows that the fuselage rigid body modes are not affected by the pitch-horn configuration. This is because no significant mast bending took place in these modes. On the other hand, the pylon mode damping is changed only slightly. This lack of sensitivity to the pitch-horn configuration on pylon mode damping was attributed to the low main rotor thrust effect and, thus, low loads in the ground resonance mode of operation.

8. Parametric Study on the Effect of Individual Mast-bending Coupling Terms on Pylon Stability.

Mast-bending coupling terms of the Model 400 for trailing-edge configuration No. 4 are presented in the following matrix. The same information was also given in Table 3.

$$\begin{bmatrix} \frac{\partial B_1}{\partial \theta_m} & \frac{\partial B_1}{\partial \phi_m} \\ \frac{\partial A_1}{\partial \theta_m} & \frac{\partial A_1}{\partial \phi_m} \end{bmatrix} = \begin{bmatrix} 0.89 & -1.05 \\ 1.05 & 0.89 \end{bmatrix} \qquad (10)$$

In order to investigate effect of the individual coupling terms on the stability characteristics of the aircraft, a parametric study was conducted using DNAW02 analysis and the dynamic parameters of Ship 3.

First, the diagonal terms of the above coupling matrix were varied from 0 to 1.6 while keeping the off diagonal terms unchanged. The results are plotted, in Fig. 19, versus rotor speed. The effects of increasing the magnitude of these coupling terms, whose direction is marked by an arrow in the figure, are a sharp reduction in damping and some increase in frequency of the pylon roll mode. It can be seen that the pylon

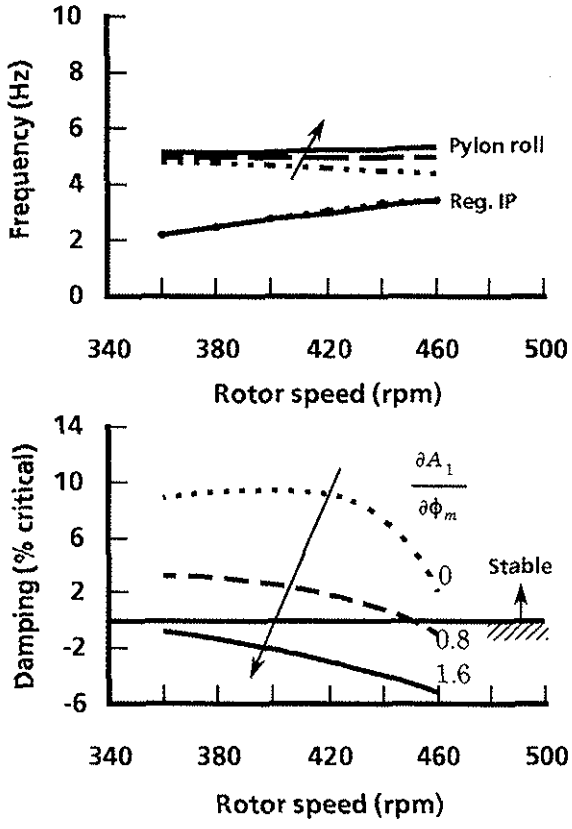

4G984

Fig. 19. Effect of magnitude of the diagonal mast-bending coupling terms on pylon roll mode stability.

roll mode goes unstable at a rotor speed where the pylon and the regressing inplane modes are well separated.

Second, the magnitude of the off diagonal terms of the coupling matrix were varied from 0 to 1.6 while keeping their sign. For this exercise, the diagonal terms were unchanged. The results are plotted in Fig. 20. The increasing magnitude of the off diagonal coupling terms also sharply decreases the pylon roll damping and reduces the pylon roll mode frequency slightly.

Increasing the magnitude of both the diagonal and the off diagonal terms of the coupling matrix has a strong destabilizing effect on the pylon roll mode damping. It should be remembered that when mast flexibility was modeled via an equivalent δ_3, the diagonal terms of the coupling matrix were excluded.

The results of this parametric study indicate that not only the sign but also the magnitude of mast-bending coupling terms has a strong effect on the pylon stability. To minimize the destabilizing effect of coupling, use of a stiff mast is suggested.

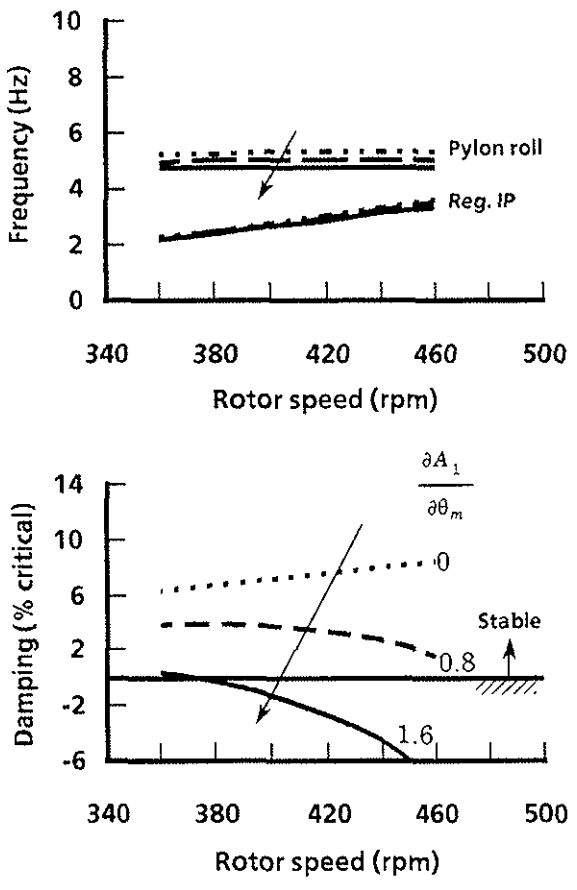

4G985

Fig. 20. Effect of magnitude of the off diagonal mast-bending coupling terms on the pylon roll mode stability.

9. Discussion on the Results

Results from analytical and experimental data indicated that mast-bending coupling with a trailing-edge pitch-horn is destabilizing on pylon damping. Examining the data revealed that the top of the mast whirls in a counterclockwise direction (as viewed from the top) when pylon instability takes place. The destabilizing mast-bending coupling tends to feather the blades in such a manner that the aerodynamic forces thus produced tend to whirl the hub in the same counterclockwise direction. This is destabilizing. Due to the fact that the rotor always lags the motion of the mast because of the high rotor inertia, a positive δ_3 would also feather the blade, tending to whirl the hub in a counterclockwise direction—which is also destabilizing. Further, for a soft dynamics system, the motion of the pylon (in a limit cycle or a diverging fashion) whirls around an ellipse with the major axis in the direction consistent with the lower pylon frequency. In the case of the Model 400, this was the pylon roll mode.

In the case of a leading-edge pitch-horn, the mast-bending coupling tends to feather the blades in such a manner that the aerodynamic forces thus produced tend to whirl the hub in a clockwise direction. This is stabilizing.

It should be noted that, although the trailing-edge pitch-horn has a destabilizing effect on pylon stability, an adequate stability margin can be achieved using a stiff mast and proper placement of the pylon frequency. This was evidenced by the data presented in Figs. 10 and 16.

10. Conclusions

1. Mast-bending coupling terms have strong effect on pylon mode damping.

2. The sign of mast-bending coupling corresponding to the trailing-edge pitch-horn configuration has a destabilizing effect on pylon modes.

3. Mast-bending coupling should be modeled separately from pitch-flap coupling to account for the hub loads.

4. Positive values of pitch-flap coupling (excluding mast flexibility) are destabilizing, especially with the trailing-edge pitch-horn configuration.

5. Acceptable pylon stability margin can be achieved with a trailing-edge pitch-horn using a stiff mast and stiff pylon mounts to minimize the magnitude of the coupling and provide sufficient frequency separation between the pylon and the regressing inplane modes.

References

1. Smith, Roger L., "An investigation of Helicopter Pylon Instability," paper presented to the Arlington State College, ASME Student Branch, Arlington, TX, May 1964.

2. Edenborough, H. K., "Investigation of Tilt-Rotor VTOL Aircraft Rotor-Pylon Stability," *Journal of Aircraft*, vol. 5.(2), March-April 1968.

3. Silverthorn, L. J. "Whirl Mode Stability of the Main Rotor of the YAH-64 Advanced Attack Helicopter," American Helicopter Society 38th Annual Forum, Washington, D.C., May 1982.

4. Kunz, Donald L., "On the Effect of Pitch/Mast-Bending Coupling on Whirl-Mode Stability," American Helicopter Society 48th Annual Forum, Washington, D.C., June 1992.

5. Loewy, Robert G., and Zotto, Mark, "Helicopter Ground/Air Resonance Including Rotor Shaft Flexibility and Control Coupling," American Helicopter Society 45th Annual Forum, Boston, MA, May 1989.

6. Perry, K. and White, J., "Testing and Correlation on An Advanced Technology, Bearingless Rotor," American Helicopter Society 44th Annual Forum, Washington, D.C., June 1988.

7. Yen, J. G., Corrigan, J. J., Schillings, J. J., and Hsieh, P. Y., "Comprehensive Analysis Methodology at Bell Helicopter: COPTER," American Helicopter Society Aeromechanics Specialists Conference, San Francisco, CA, January 1994.